Extinction controlled Adaptive Mask Coronagraph Lyot and Phase Mask dual concept for wide extinction area

P. Bourget*, N. Schuhler,D. Mawet, P. Haguenauer, Girard, J., Gonte, F.
European Southern Observatory, Alonso de Córdova 3107- Vitacura, Santiago, CHILI

ABSTRACT

A dual coronagraph based on the Adaptive Mask concept is presented in this paper. ALyot coronagraph with a variable diameter occulting disk anda nulling stellar coronagraph based on the Adaptive Phase Mask concept using polarization interferometry are presented in this work. Observations on sky and numerical simulations show the usefulness of the proposed method to optimize the nulling efficiency of the coronagraphs. In the case of the phase mask, the active control system will correct for the detrimental effects of image instabilities on the destructive interference (low-order aberrations such as tip-tilt and focus). The phase mask adaptability both in size, phase and amplitude also compensate for manufacturing errors of the mask itself, and potentially for chromatic effects. Liquid-crystal properties are used to provide variable transmission of an annulus around the phase mask, but also to achieve the achromatic π phase shift in the core of the PSF by rotating the polarization by 180º.A compressed mercury (Hg) drop is used as an occulting disk for the Lyot mask, its size control offers an adaptation to the seeing conditions and provides an optimization of the Tip-tilt correction.

Keywords:high-contrast imaging, coronagraphy, polarization, high angular resolution, phase mask, adaptive optics

1. INTRODUCTION

The Adaptive Mask Coronagraph using "non-solid" masks was developed to improve coronagraphs observational efficiency (Bourget et al. 2004). The first issue of this concept was the Hg-mask Lyot coronagraph dedicated to an astrometric survey of faint satellites near Jovian planets (Bourget et al. 2001),(Vieira Martins et al. 2004) and (Veiga& Bourget, 2006).To optimize the occulting process of theLyot coronagraph, a compressed mercury (Hg) drop is used as an occulting disk and its size control offers an adaptation to the seeing conditions or to the required fraction of the Airy diameter.

To achieve high contrast imaging within a small angular separation, not allowed by the Lyot coronagraph, an adaptive phase mask was developed following theRoddier&Roddiercoronagraph concept (Roddier&Roddier1997).The nulling efficiency provided by a classical phase mask is strongly dependent on the amplitude balance of the two phase shifted waves. The principal factors contributing to the unbalance of the amplitudes are: the chromaticity of the Airy disk diameter (i.e of the phase mask diameter), the image centering stability on the mask and the Strehl ratio. The optimal phase mask diameter is essentially wavelength and bandwidth dependent and must be controlled with high accuracy; it can also depend on the pupil apodization technique used (Guyon al. 2006). Even using an adaptive optics correction, the residual low order aberrations will impact the centering and the Airy pattern shape. Instead of acting on the amplitude misbalance causes, we propose to actively balance the amplitudes by modulating the transmission of the area outside of the phase mask. The control loop error signal is obtained by a direct measurement of the nulling efficiency with an avalanche photodiode at the coronagraph output. The optical modulation is done by the means of liquid-crystal polarization properties also used to produce the π phase shift.

*pbourget@eso.org; phone: (56) 5543 5378

Modern Technologies in Space- and Ground-based Telescopes and Instrumentation II,
edited by Ramón Navarro, Colin R. Cunningham, Eric Prieto, Proc. of SPIE Vol. 8450, 84505I
 · doi: 10.1117/12.927284

An Hg-Mask Lyot coronagraph and an Adaptive Phase Mask Roddier&Roddier coronagraph working simultaneously in two perpendicular linear polarizations compose the instrument concept. The Hg-Mask coronagraph offers the high dynamic range imaging at large angular separation and also provides the tip tilt correction system already developed for a precedent instrument (Bourget et al. 2004). The Adaptive Phase Mask coronagraph uses a variable diameter liquid-crystal phase mask with modulation of the transmission in the external part of the core. A two-stage adaptive phase mask following the Multi-Stage Vortex Coronagraph concept (Mawet et al. 2004) is also presented for high contrast imaging using an on-axis telescope.

2. THE Hg-MASK LYOT CORANAGRAPH

2.1 The Hg-Mask

The use of an ever-finite numbers of fixed-diameter occulting disks makes difficult the Lyotcoronagraphy. In fact, difficulties appear when changing the disk during observations since it has not often the good size and need to be centered with appropriate offsets. We proposed a solution to this problem by using mercury to realize variable diameter occulting disks. We take into account the high density of the mercury by its superficial tension that allows making a spherical drop with an optical quality. The drop is glued between optical windows by the Van Der Waals forces and is used as the occulting disk (see figure 1). In a Lyotcoronagraphic process the occulting mask acts on the scattered light as all the optical elements. The phase errors produced by the optical roughness of both (optics and mask) induce the scattered light (”Halo”). The minimum of the surface tension potential function provides a toric free surface of mercury physically perfect (λ /100). The control of the distance between the optical windows acts on the tore diameter with a sub micron-precision. The three dimensional occulting process on the tore induces an apodization of the occultation. The diameter limits are 10 microns to 1.5 millimeters with different ranges of mercury drops compression. The surface of the tore is locally perfect and provides high diffraction quality of the occulting disk.

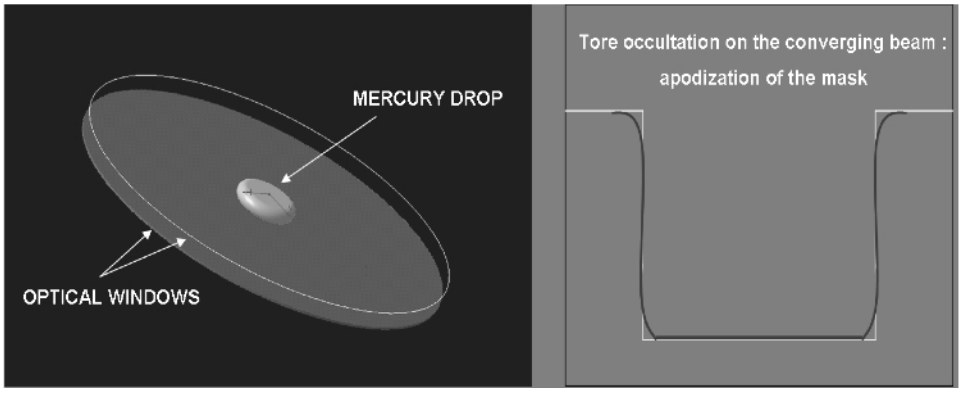

Figure 1. Hg Mask: The distance between the optical window and the pellicle film induces the size control of the toric free surface of mercury.The game between the surface tension and the Van Der Waals forces provides the control of the small tore radius: this radius will be smaller compressing the mercury and will increase if the compression is slightly released because the van der Walls forces are stronger. This allowsfine-tuning of the diffraction quality.

2.2 Automatic centering and tip-tilt correction

The centering and the stability of the object behind the mask are critical parameters for the coronagraph efficiency. The diffraction effect produced by the centering instability is highly dynamic and provides an efficient pointing error signal. The dynamic of this signal allow high SNR and was already used to realize an automatic centering and tip-tilt correction system for the instrument developed at the National Observatory of Brazil(figure 2).The decentering detection is done by a four-quadrant photodiode placed at the output of the coronagraph. A pellicle beam splitter is placed before the scientific detector to feed the four-quadrant. When the control loop is closed for the tip-tilt correction, the Hg-mask diameter starts also to be controlled: the minimization of the pointing signal “variance”is done by a control of the Hg-Mask diameter. After minimizing the “variance”, the “gain” of the tip-tilt control loop is increased at the limit. This process optimizes the control loop parameters to the seeing conditions, or residual adaptive optics correction, and also provides an automatic centering for the coronagraph.

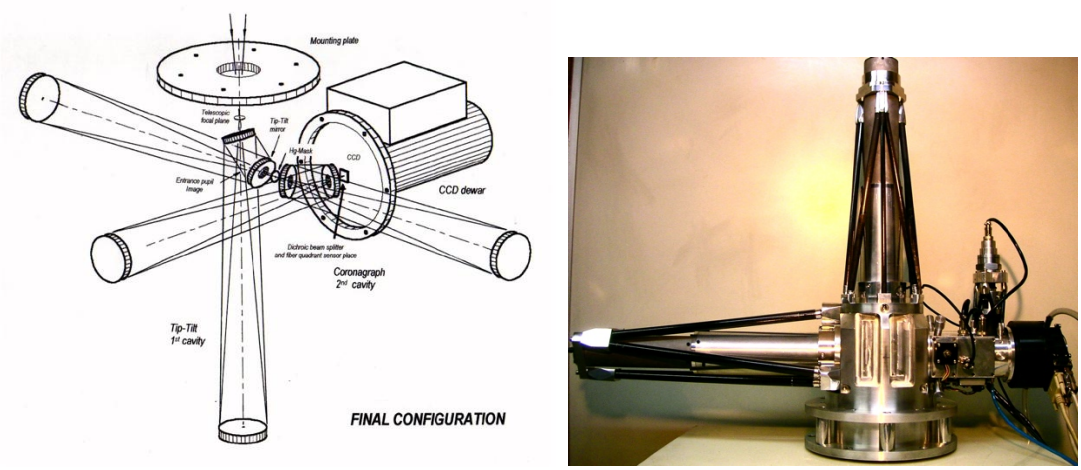

Figure 2. The final configuration on the left was projected with a complete reflective optics. The tip-tilt mirror is placed at the pupil image plane on the first cavity. At the output, the Hg-Mask is inserted and the coronagraph optics is completely symmetric to the tip-tit cavity. A variable diameter Lyot diaphragm is mounted at the pupil image inside the coronagraph. A pellicle beam splitter is placed before the scientific detector to feed the APD four-quadrant.The first prototype of the tip-tilt correction system is on the right; the coronagraph stage is the astrometric survey instrument with a refractive optics. The tip-tilt sensor uses an image intensifier feeding a classical four-quadrant photodiode.

3. THE ADAPTIVE PHASE MASK CORANAGRAPH

3.1 The adaptive Phase Mask

The first Adaptive Phase Mask was made of a gas bubble immersed ina layer of oil between two optical windows. The phase delay φ of the Airy pattern core on the focal plane was obtained by refraction (figure 3).

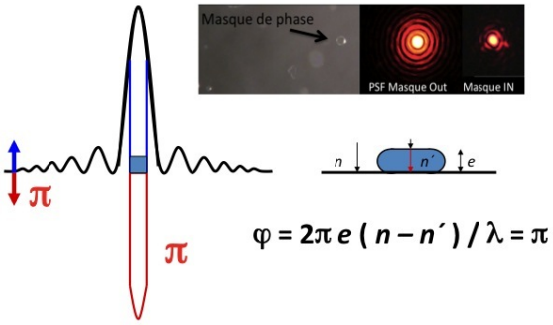

Figure 3.n and n′ are respectively the refractive index of the liquid and of the bubble, e is the distance between the optical windows and λ the observation wavelength. Typical values for n and n′ are respectively about 1.5 and 1 leading to a controlled delay e ≈ kλ where k is an integer. Since the variation of the retardation is a linear function of e and the diameter varies with e-1/2, the distance e allows controlling either chromatism or the diameter. As a consequence the gas bubble mask works only over a narrow wavelength bandwidth.

The phase-shift done by refraction, strongly chromatic, is done by the thickness of the bubble. Calibrated micro spheres inside the crystal-liquid were used to calibrate the thickness then the spectral bandwidth of each adaptive phase mask. The complexity to obtain the exact bubble diameter size and the chromatism were the essentials limitations to provide high contrast efficiency during the first tests carried out at the Rio de Janeiro National Observatory – Brazil (Bourget et al. 2004).

A solution to those limitations is presented using a “geometrical” phase shift (Pancharatnam 1956; Berry 1987). Instead of a phase delay induced by the refraction, a “geometrical” phase shift is realized by rotation of the polarization exploiting the properties of liquid-crystals. The “twisted nematic or cholesteric” liquid crystals are used to rotate the polarization of the incident light. The liquid crystal is used between to perpendiculars linear polarizers. An achromatic π phase shift between the core of the PSF and the external region is achieved by rotating the polarizations. The central zone is phase shifted by $+\pi/2$ and outside the polarization is rotated around $-\pi/2$ so that the second polarizer stops the required amount of light (figure 4).

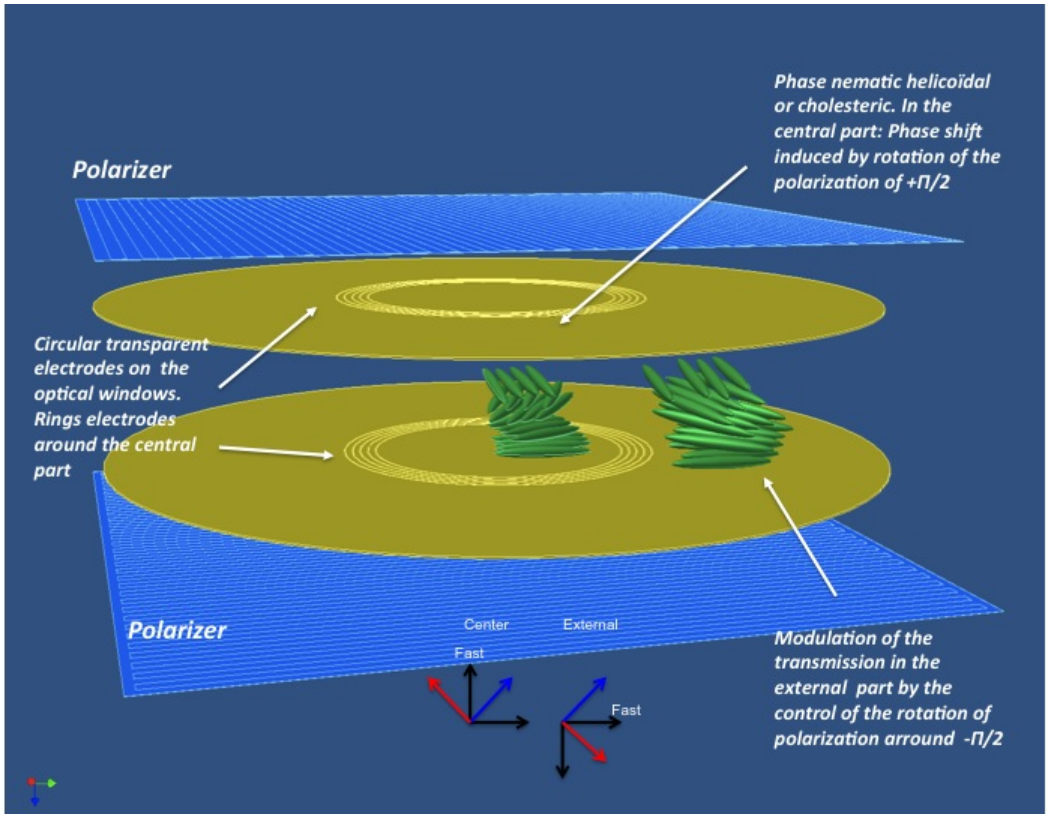

Figure 4.In the bottom of the figure the dark arrow (45º) represent the polarization at the entrance of the phase mask and the clear arrow the state of polarization at the output; the twisted nematic orientation provides the perpendicularity of the fast axis.

The phase mask diameter is smaller than needed to provide the 50% theoretical balance of shifted phase amplitudes with a full transmission, the extinction control system will maintain the balance and the nulling efficiency by decreasing the transmission outside of the central core. The phase mask efficiency is then always at a maximal level. If the phase mask diameter is decreased, the extinction control will allow observing much closer to the central star but at the cost of an increasing exposure time. An angular separation scanning close to the central star is allowed by the adaptive phase mask. This scanning facility will allow fine-tuning of the nulling efficiency depending on the conditions of observation. Circular concentric electrodes can provide a step-by-step variable diameter of the inner region. The transition in the electric field will introduce a discontinuity in the polarization; the effect of the discontinuity needs to be quantified experimentally. Baba et al. in 2002 and Murakami et al. in 2010 have already presented successful liquid-crystal applications for coronagraphs and especially the eight-octant phase mask (EOPoM). Even penalized by a 10µm gap between the eights octants, the peak extinction level of 3.10-4 reached by the EOPoM provides an realistic reference for our future experiments, especially since the Adaptive Phase Mask do not present a central dead zone.

3.2 Nulling detection and control loop:

The nulling efficiency detection is done using an avalanche photodiode (APD) at the output of the coronagraph. As for the Hg-Mask coronagraph tip-tilt correction, a pellicle beam splitter is placed before the scientific detector to feed a single APD and not a four quadrant (Figure 5):a tip-tilt error degrades the amplitudes balance of the two shifted waves, the active control of the balance is independent of the tilt direction, the modulation of the transmission outside of the phase mask is uniform.As the phase mask diameter is smaller than needed to provide the 50% theoretical balance with a full transmission,the flux measured by the APD willreach a minimum decreasing the transmission outside of the phase mask,and increase again. This minimum will correspond to the amplitude balance of the two shifted waves and also to the best nulling; this value will be used as a reference for the control loop on the transmission. If the value measured by the APD is higher than the reference one, the control loop will decrease the transmission outside of the phase mask to minimize the flux measured by the APD. As an over correction will increase the flux measured by the APD, the "nulling" control loop is done on a stability point. The extinction control system will maintain the nulling efficiency to an optimal value. High band pass control is provided by the APD and Liquid-crystals properties.

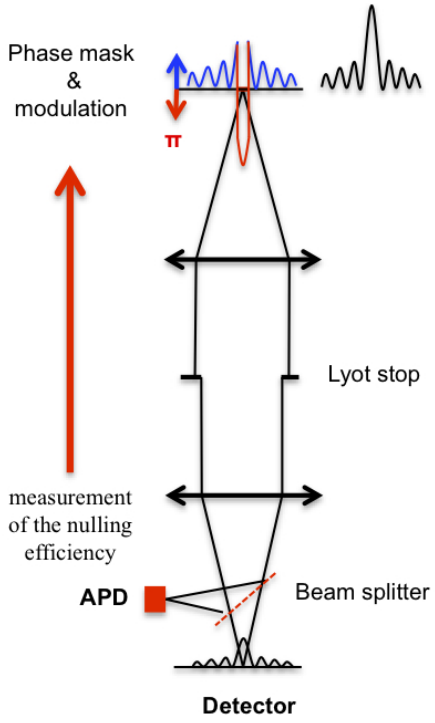

Figure 5.Adaptive Phase Mask coronagraph layout

3.3 Sensitivity to the Tip-Tilt

The centering error of the Airy pattern on the phase mask produces a misbalance of the amplitude of the two phase shifted waves, the flux transmitted outside of the phase mask is increased. The optimization of extinction, which decreases the transmission, tends to balance the amplitudes of the phase-shifted waves. Nevertheless the destructive interference that will occur in the pupil plane is spatially dependent on the pupil energy distribution for both waves. The centering error induces a different energy repartition that will prevent the total destructive interference. Using the Matrix Fourier Transform method presented in Soummer et al. 2007, our numerical simulations were done to quantify the range of efficiency of the transmission control system over an increasing Tip-Tilt error. The centering error of the Airy pattern on the adaptive phase mask was introduced in the simulation by a Tilt of the incoming wave front. The optical setup for the following simulation is without central obstruction.

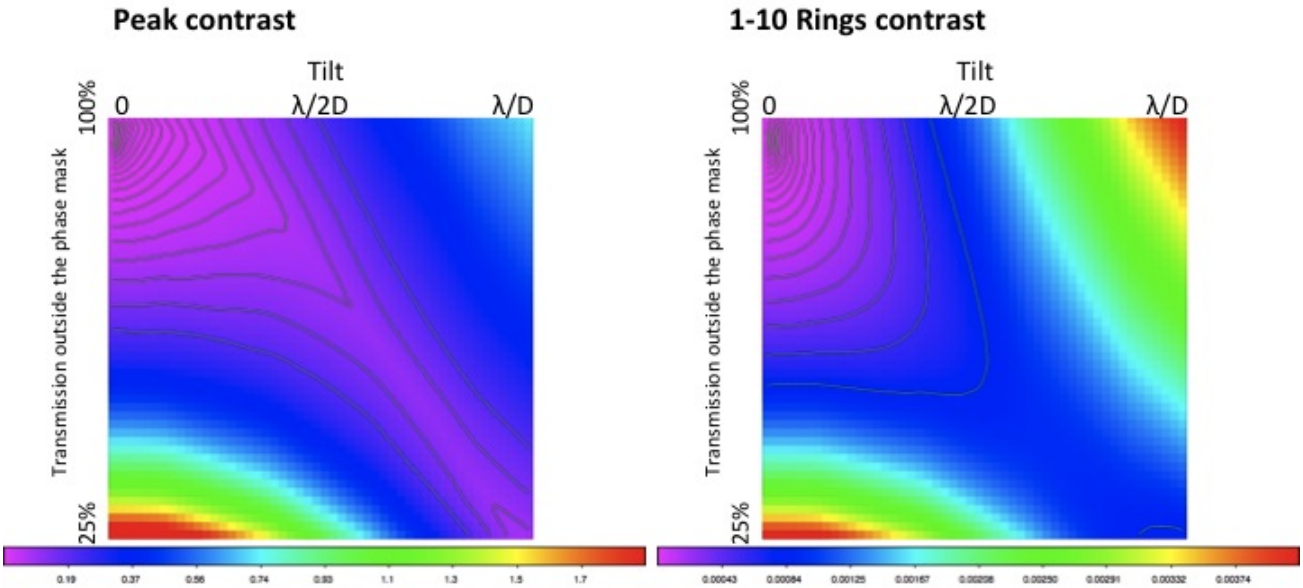

Figure 6.The horizontal axis of the figures 6&7 is the tip-tilt error from 0 until λ/D. The vertical axis is the transmission outside of the phase mask. The figure represent the color map of the contrast for the peak of the Airy pattern on the left side, and for the rings from the first until the 10th on the right side. The phase mask diameter is 0.5 λ/D: slightly smaller than the one that will provide a perfect theoretical balance. Numerical simulation shows that the nulling efficiency of the phase mask is maintained by a 95% transmission outside of the phase mask, the transmission control allow fine tuning of contrast. The increasing tilt error effect on the contrast is partially removed by a diminution of the transmission as shown by the color map.

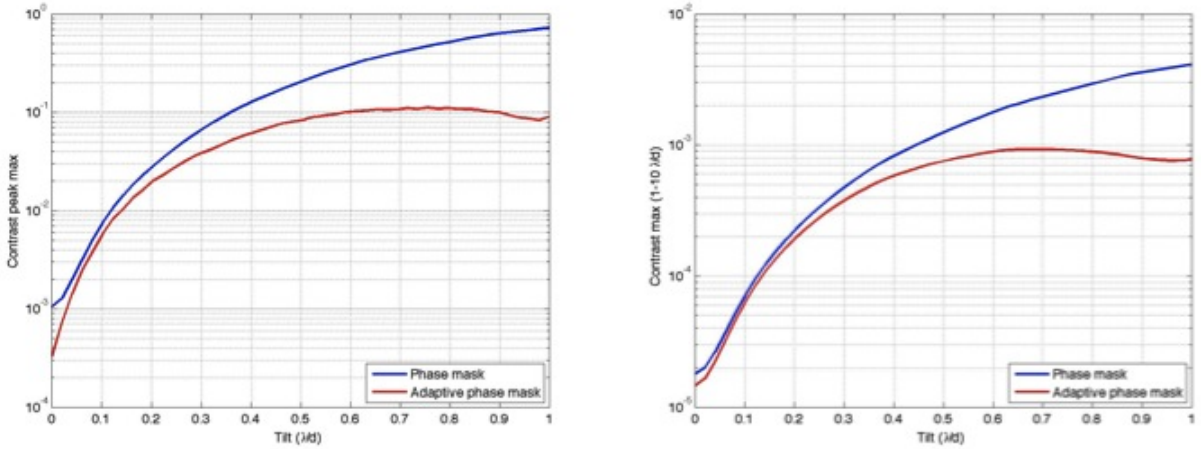

Figure 7.The vertical axis is the contrast reached by the coronagraph. The blue curve represents the variation of the contrast without any control of transmission outside of the phase mask (first upper line of the figure 4). The contrast of the peak of the Airy pattern is on the left side and for the rings on the right side from the first until the 10th. The red curve illustrates the contrast achieved by the control of transmission with an increasing tilt. The best achievement of the transmission control system is obtained on the rings where the contrast is needed and stays bellow 1.10-3 with a tilt of λ/D.

3.4 Micro tip-tilt compensation

In the pupil plane, the non-uniform energy repartition of both waves that prevent the total destructive interference will decrease if the transmission control is sectorized in four quadrants (figure 8). In that case a four quadrant APD is needed to provide the transmission control signal to each quadrant of the focal plane electrode around the phase mask. Complementary simulations were done using classical Fourrier transform to quantify the improvement of the proposed

technique for the tilt compensation. The optical setup for those simulations is:1/8 for the central obstruction and f/30 focal ratio for the incoming beam.

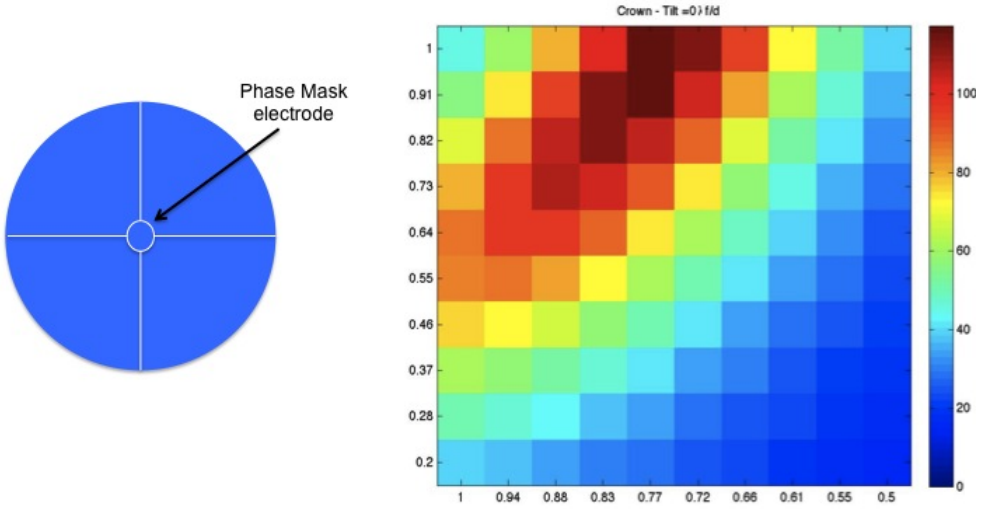

Figure 8.For the simulations the focal plane is divided in half perpendicularly to the tilt direction. The results are presented on the figures 8&9. The horizontal axis represents the transmission of the part opposite to the tilt direction. On this axis the transmission start from 100% until 50%. The vertical axis represents the transmission of the other part as a fraction of the first one. The color scale is to be considered as relative and not absolute extinction. On the first upper line the variation of transmission of both part is identical because the fraction factor is one. For other horizontal line the transmission in the tilt direction part is the one of the opposite part multiplied by the fraction factor of the line.

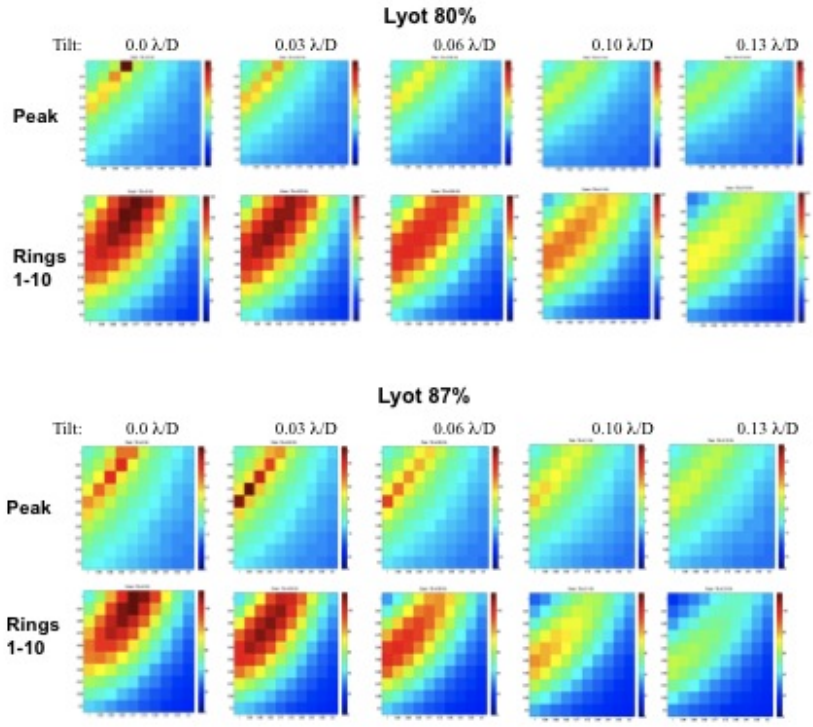

Figure 9.The color map of extinction is presented for each value of tilt error. This series of figures shows that a sectorized adaptive phase mask is more efficient than the uniform one for an increasing tilt error bellow 0.13 λ/D, this is at the cost of an higher SNR of the four quadrants APD compared to the single APD. A calibration is also necessary to avoid any kind of coupling.

3.5 Two stage Adaptive Phase Mask

In the case of a Lyot coronagraph, the occulting mask diffraction injects high frequencies inside the pupil image and especially on the border of the pupil. The Lyot diaphragm is used to stop that diffraction effect allowing high contrast imaging but at the cost of a loss of flux and resolution. For an on-axis telescope, the central obstruction introduces a diffraction effect that will also inject high frequencies inside the pupil image of the central obstruction; this contribution will easily be suppressed by a stop placed on the central obstruction image without loosing flux. For a phase mask coronagraph, the distribution of the high frequencies due to the diffraction on the mask is inverted compared to the Lyot coronagraph. High frequencies are rejected outside of the pupil image; a Lyot diaphragm stops them without loosing flux and resolution, the pupil size is unchanged. Nevertheless, a central obstruction will introduce high frequencies outside its pupil image then inside the useful pupil. As described by Haguenauer et al. 2005, the contribution of the central obstruction will strongly affect the efficiency of the interference process. Using a Four-Quadrant Phase Mask (Rouan et al. 2000), numerical simulations shows that a 1,5m sub-pupil of the Palomar telescope (without central obstruction) allows reaching higher contrast than with the entire 5,1m pupil (with central obstruction).

The Multi-Stage Vortex Coronagraph concept, developed by Mawet et al. 2011, proposes a method to significantly attenuate the contribution of the diffraction induced by the central obstruction. Using the optical properties of the Vector Vortex Coronagraph (Mawet et al. 2005), the high frequencies injected in the pupil by the central obstruction can be removed by a stop without loosing light in a second stage of vortex coronagraphs. This action is allowed if the phase ramp of the two Vortex are inverted; in that casethe high frequencies injected in the pupil by the central obstruction are transferred inside the central obstruction image in the second stage of coronagraph and then stopped by a mask. Following the Multi-Stage Vortex Coronagraph concept, the axisymmetric action of the two stages Vortex is applicable to other phase masks such as the four quadrants phase mask (FQPM) and the Roddier&Roddier phase mask. The numerical simulation of a two-stage phase mask coronagraph with a π phase shift inverted at each image plane was performed to verify the diffractions effects of the central obstruction for an on-axis telescope (figure 10).

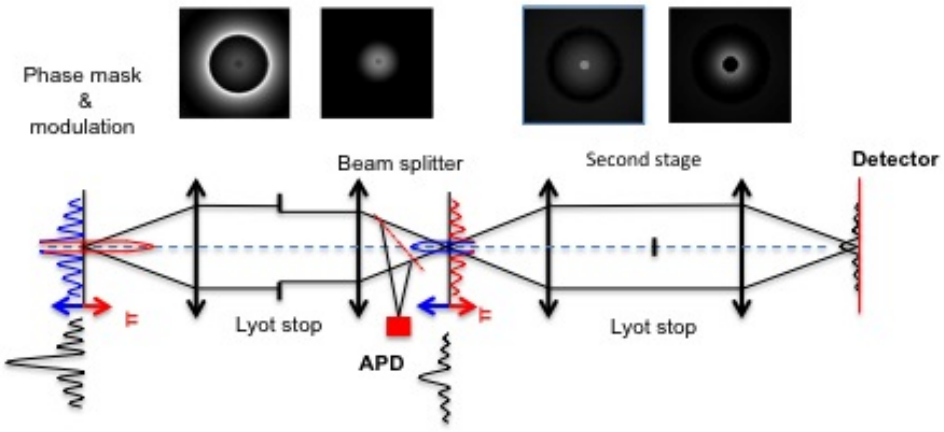

Figure 10. On the first adaptive phase mask, the phase shift is obtained by rotation of the polarization as shown figure 4. The control loop on the transmission outside of the phase mask is done at the first stage of the coronagraph. At the second stage, the adaptive phase mask applies the rotation of polarization reverse. The sense of the twists is exchanged at the second stage. On the upper part appear the pupils before and after the pupil Lyot stop for each stage. The diffraction effects on the masks are rejected outside of the pupil "contour" image at the first stage and inside the pupil "contour" image at the second stage. The remnant flux around the central obstruction image at the first stage is injected inside the central obstruction image at the second stage. The detection of the nulling by the APD is done at the output of the second stage. The second adaptive mask is passive, its effect on the destructive interference need to be taken into account by the APD during the optimization of the nulling before closing the loop.

4. LYOT AND PHASE MASK DUAL CONCEPT

A dual coronagraph based on the Adaptive Mask concept can allow observing with high contrast at a large angular scale and simultaneously within a small angular separation.

TheLyotHg-Mask coronagraph provides high contrast imaging at a large angular separation. The astrometric survey of the Neptune and Uranus respective satellites Proteus and Puck obtained a direct dynamic imaging of 14.5 ΔV-Mag at 3,5 arc second from the border of the planet. These results were obtained in the visible wavelength, without adaptive optics, at the 1.6m diameter telescope from the National Laboratory of Astrophysics of Brazil (LNA), [15,16].Thiscapability of extinction of the Hg-Mask Lyot coronagraph was already tested for the Beta Pictoriscircumstellar disk and gave an optimistic reference for future observations using an adaptive optics correction. The Hg-Mask coronagraph will also provide the tip-tilt correction signal and the automatic centering system already developed and presented section 2.2.

To achieve simultaneously high contrast imaging within a small angular separation, not allowed by the Lyot coronagraph, the adaptive phase mask will work in the two stage concept if working with a central obscuration as presented bellow figure 11.

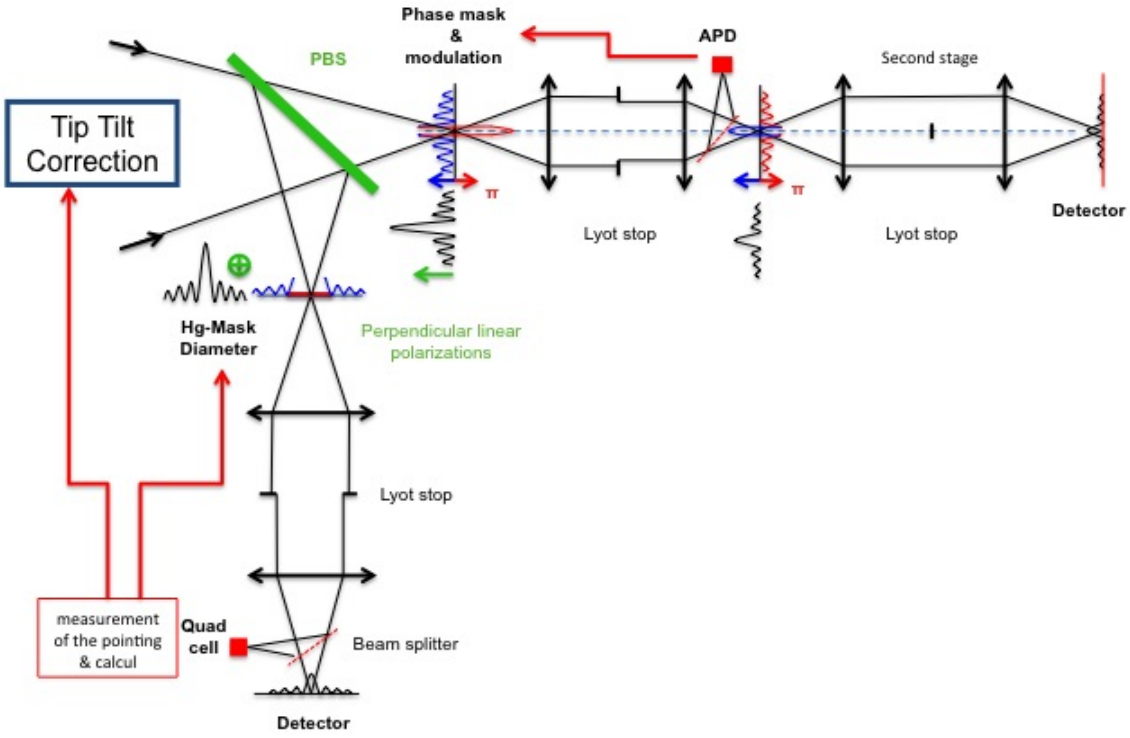

Figure 11. The pointing signal obtained by the diffraction signal coming from the Hg-Mask is used for the tip-tilt correction and automatic centering. The minimization of the pointing signal "variance" done by the control of the Hg-Mask diameter optimizes the control loop parameters to the seeing conditions and residual adaptive optics corrections. After minimizing the "variance", the "gain" of the tip-tilt control loop is increased. The nulling efficiency that provides the phase mask is strongly dependent on the amplitude balance of the two phase shifted waves, then we propose to actively balance the amplitudes by modulating the transmission of the area outside of the phase mask. The control loop error signal is obtained by a direct measurement of the nulling efficiency with an avalanche photodiode at the coronagraph output. The optical modulation is done by the means of liquid-crystal polarization properties also used to produce the π phase shift.

5. CONCLUSIONS AND PERSPECTIVES

This paper presented the innovative concept of Adaptive Phase Mask, which was shown toallow an active optimization of the nulling process of a Lyot coronagraph and Roddier&Roddier disk phase mask coronagraph. In this first paper, we focused on the active control of the effects of both the phase-mask diameter with respect to wavelength, and the image instabilities (tip, tilt, …). High band pass control is provided by the APD and Liquid-crystals properties.The chromatic effect of the phase shift is minimized using the "geometrical phase" (Pantcharatnam 1956, Berry 1987). The flexibility introduced by the geometric phase and the use of liquid crystals is thus very promising regarding adaptability of the

mask in both size and phase. Note that more complex phase and amplitude profiles could also be rendered to implement adaptable versions of the dual zone phase mask coronagraph (N'Diaye et al. 2012). In the case of an on-axis telescope, the central obstruction diffraction effect is strongly decreased by a two-stage coronagraph following the two-stage Vortex coronagraph concept developed by Mawet et al. 2011. The experience acquired with the Hg-Mask Lyot coronagraph development allows providing a wide extinction area instrument by a dual adaptive mask concept.

Acknowledgements. This work was carried out at the European Southern Observatory (ESO) site of Vitacura (Santiago, Chile).

REFERENCES

[1] Baba, N., Murakami, N., Ishigaki, T., & Hashimoto, N., Optics Letters, 27, 1373, (2002).

[2] Berry, M. V., Journal of Modern Optics, 34, 1401, (1987).

[3] Bourget, P., Veiga, C. H., & Vieira Martins, R., PASP, 113, 436, (2001).

[4] Bourget, P., Veiga, C. H., Vieira Martins, R., Assus, P., & Colas, F., "Astronomywith High ConstrastImaging II", in EAS Publications Series ed.,Vol. 12, 205, (2004).

[5] Bourget, P., Vieira Martins, R., Colas, F., Assus, P. &Irbah, A., Proceedings IAU Colloquium 200, 461-465, (2006).

[6] Guyon, O., Pluzhnik, E. A., Kuchner, M. J., Collins, B., & Ridgway, S. T., ApJS, 167, 81, (2006).

[7] Haguenauer, P., Serabyn, E., Bloemhof, E. E., et al., in Society of Photo-Optical Instrumentation Engineers (SPIE)Conference Series, Vol. 5905, Society of Photo-Optical Instrumentation Engineers (SPIE) Conference Series, ed. D. R.Coulter, 261–271, (2005).

[8] Mawet, D., Riaud, P., Absil, O., &Surdej, J., ApJ, 633, 1191, (2005).

[9] Mawet, D., Serabyn, E., Wallace, J. K., &Pueyo, L., Optics Letters, 36, 1506, (2011).

[10] Murakami, N., Nishikawa, J., Yokochi, K., et al., ApJ, 714, 772, (2010).

[11] N'diaye, M., Dohlen, K., Cuevas, S., et al., A&A, 538, A55, (2012).

[12] Pancharatnam, S., Proc. Indian Acad. Sci., 44, 247, (1956).

[13] Roddier, F. &Roddier, C., PASP, 109, 815, (1997).

[14] Rouan, D., Riaud, P., Boccaletti, A., Clénet, Y., &Labeyrie, A., PASP, 112, 1479, (2000).

[15] Veiga, C. H. & Bourget, P., A&A, 454, 683, (2006).

[16] Vieira Martins, R., Veiga, C. H., Bourget, P., Andrei, A. H., &Descamps, P., A&A, 425, 1107, (2004).